Neuron
Article

Closed-Loop Deep Brain Stimulation Is Superior in Ameliorating Parkinsonism

Boris Rosin,[1,*] Maya Slovik,[1] Rea Mitelman,[1,2] Michal Rivlin-Etzion,[1,2] Suzanne N. Haber,[3] Zvi Israel,[4] Eilon Vaadia,[1,2,5] and Hagai Bergman[1,2,5]
[1]Department of Medical Neurobiology (Physiology), The Institute for Medical Research Israel-Canada, The Hebrew University-Hadassah Medical Association School of Medicine and Hadassah University Hospital, Jerusalem 91120, Israel
[2]The Interdisciplinary Center for Neural Computation, Givat Ram Campus, The Hebrew University of Jerusalem, Jerusalem 91904, Israel
[3]Department of Pharmacology and Physiology, School of Medicine and Dentistry, University of Rochester, Rochester, NY 14642, USA
[4]Center for Functional & Restorative Neurosurgery, The Hebrew University-Hadassah Medical Association School of Medicine and Hadassah University Hospital, Jerusalem 91120, Israel
[5]The Edmond & Lily Safra Center for Brain Sciences, Givat Ram Campus, The Hebrew University of Jerusalem, Jerusalem 91904, Israel
*Correspondence: boris.rosin@mail.huji.ac.il
DOI 10.1016/j.neuron.2011.08.023

SUMMARY

Continuous high-frequency deep brain stimulation (DBS) is a widely used therapy for advanced Parkinson's disease (PD) management. However, the mechanisms underlying DBS effects remain enigmatic and are the subject of an ongoing debate. Here, we present and test a closed-loop stimulation strategy for PD in the 1-methyl-4-phenyl-1,2,3,6-tetrahydropyridine (MPTP) primate model of PD. Application of pallidal closed-loop stimulation leads to dissociation between changes in basal ganglia (BG) discharge rates and patterns, providing insights into PD pathophysiology. Furthermore, cortico-pallidal closed-loop stimulation has a significantly greater effect on akinesia and on cortical and pallidal discharge patterns than standard open-loop DBS and matched control stimulation paradigms. Thus, closed-loop DBS paradigms, by modulating pathological oscillatory activity rather than the discharge rate of the BG-cortical networks, may afford more effective management of advanced PD. Such strategies have the potential to be effective in additional brain disorders in which a pathological neuronal discharge pattern can be recognized.

INTRODUCTION

Parkinson's disease (PD) is a highly debilitating and prevalent neurodegenerative disorder characterized by both motor and nonmotor symptoms (van Rooden et al., 2011), with the former mainly including muscle rigidity, 4–7 Hz rest tremor and akinesia (Zaidel et al., 2009). Human patients with advanced PD are often treated by DBS, which can alleviate the disease's motor symptoms (Benabid et al., 2009; Bronstein et al., 2011; Weaver et al., 2009). This procedure consists of implanting a multicontact macroelectrode, typically in either the internal segment of the globus pallidum (GPi) or the subthalamic nucleus (STN; Follett et al., 2010; Moro et al., 2010), and the application of constant high-frequency (approximately 130 Hz) stimulation. The stimulation parameters (e.g., frequency, pulse width, and intensity) are determined by a highly trained clinician and the initial programming can take up to 6 months before obtaining optimal results (Bronstein et al., 2011; Volkmann et al., 2006). Subsequently, the stimulation parameters are adjusted intermittently every 3–12 months during the patient's visits to the neurology clinic (Deuschl et al., 2006). The goal of the stimulator programming is to adjust the DBS parameters in order to achieve an updated optimal trade-off between maximization of clinical improvement and minimization of stimulation-induced side effects. The parameters usually remain unchanged between clinical adjustments and the resulting stimulation is thus poorly suited to cope with the dynamic nature of PD. Indeed, both the neuronal discharge of the BG in PD patients and MPTP-treated primates and the parkinsonian motor symptoms display considerably faster dynamics than those provided by the adjustments of DBS therapy (Brown, 2003; Deuschl et al., 2006; Hammond et al., 2007; Moro et al., 2006; Raz et al., 2000). Additionally, more frequent parameter adjustments have been shown to improve DBS efficacy (Frankemolle et al., 2010; Lee et al., 2010; Moro et al., 2006). This highlights the need for an automatic and dynamic system that can continually adjust the stimulus to the ongoing neuronal discharge. In recent years, the role of pathological discharge patterns in the parkinsonian brain has emerged as pivotal in the disease pathophysiology (Eusebio and Brown, 2007; Hammond et al., 2007; Kühn et al., 2009; Tass et al., 2010; Vitek, 2008; Weinberger et al., 2009; Wichmann and DeLong, 2006; Zaidel et al., 2009). Thus, such automatic systems should aim to disrupt these pathological characteristics (e.g., pattern, rate) of the neuronal discharge (Feng et al., 2007; Tass, 2003).

Considerable effort has been made toward understanding the pathophysiology of PD and the mechanisms by which DBS brings about clinical improvement. With regard to PD pathophysiology, the intermittent neuronal oscillations in the basal ganglia of PD patients and the basal ganglia and the primary motor cortex (M1) of MPTP-treated primates have been described on numerous occasions (Goldberg et al., 2002; Hurtado et al., 2005; Kühn et al., 2009; Levy et al., 2002; Raz et al., 2000).

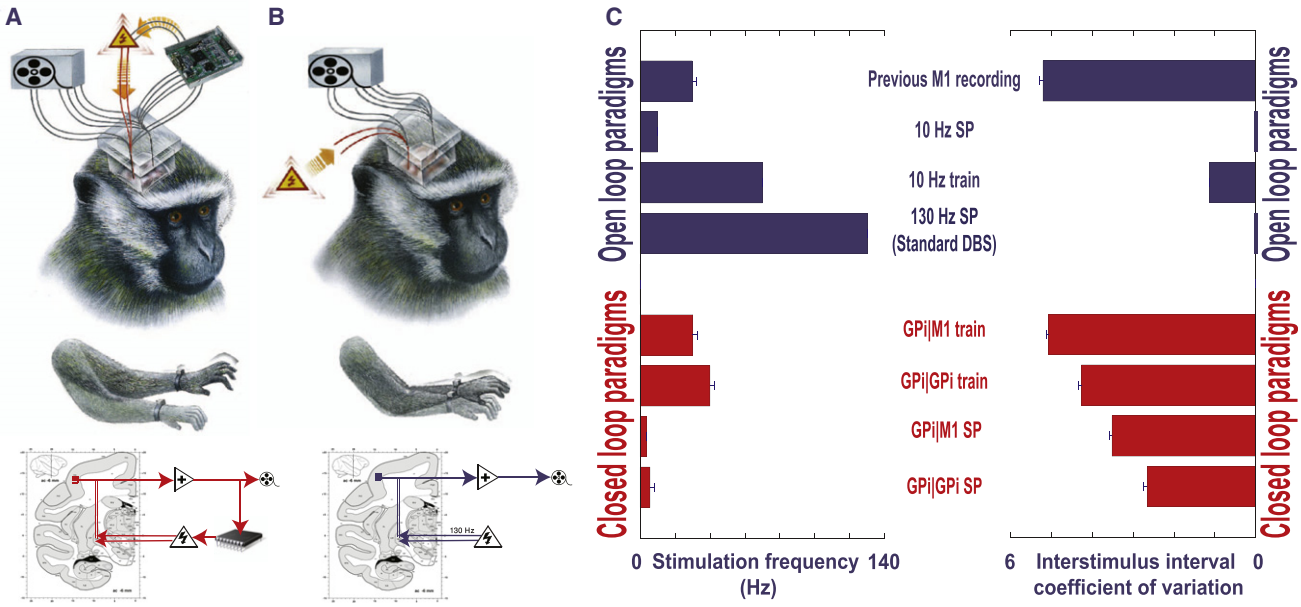

Figure 1. The Different Stimulation Paradigms and Their Characteristics

(A) Schematic representations of the closed-loop experimental paradigms. The analog signal of the six recording electrodes (2 GPi, 4 M1) is amplified and fed into a data acquisition system and a Digital Signal Processing (DSP) chip, which uses one of these channels as a reference for trigger identification. A stimulus (either single pulse or train) is delivered through the two stimulating electrodes (GPi) following identification of a trigger with a delay set by the user (80 ms in this study).

(B) Schematic representations of the standard open-loop 130 Hz GPi DBS experimental paradigm. The stimulus is delivered through the stimulating electrodes according to a predefined scheme regardless of the ongoing neuronal activity. Data acquisition settings are as in the closed-loop paradigms.

(C) The stimulation frequency (Hz; left bar chart) and the coefficient of variation (CV, standard deviation divided by the mean; right bar chart) of the interstimulus intervals for the various stimulation paradigms. Open-loop paradigms are shown in blue, closed-loop paradigms in red. Error bars indicate SEM. Differences in the resulting stimulation frequencies were statistically significant (one-way ANOVA, $p < 0.01$, Bonferroni adjusted), except when comparing $GP_{train}|M1$ closed-loop paradigm and the nonadaptive stimulation based on the previous M1 recording control paradigm. Coronal section image in subplots A and B reprinted from *Primate Brain Maps: Structure of the Macaque Brain*, H. Nakamura, copyright 2000, with permission from Elsevier.

However, the role of these oscillations as the neuronal correlate of PD motor symptoms is still debated (Hammond et al., 2007; Leblois et al., 2007; Lozano and Eltahawy, 2004; McIntyre et al., 2004; Tass et al., 2010; Vitek, 2002; Weinberger et al., 2009). In MPTP-treated primates this oscillatory activity appears to be concentrated in distinct frequency bands, including a tremor frequency band (4–7 Hz, theta band) and a double-tremor frequency band (9–15 Hz, alpha band; Bergman et al., 1994; Raz et al., 2000). Previous studies examining the effect of DBS on ongoing neuronal discharge patterns have been inconclusive, with some pointing toward disruption of presumably pathological neuronal patterns (Bar-Gad et al., 2004; Carlson et al., 2010; Deniau et al., 2010; McCairn and Turner, 2009), while others suggesting focal inhibition (Dostrovsky et al., 2000; Lafreniere-Roula et al., 2010). Better understanding of PD pathophysiology, the mechanisms by which DBS exerts its clinical effects, and the interaction between the two is thus clearly crucial to devise better treatment strategies.

In this article, we test several novel paradigms for real-time adaptive (closed-loop) deep brain stimulation in the vervet MPTP model of Parkinson's disease. We show that some closed-loop paradigms ameliorate parkinsonian akinesia and reduce abnormal corticobasal ganglia discharge better than standard DBS and other matched open-loop paradigms. Moreover, other closed-loop paradigms differentially modulate discharge rate and oscillatory activity, and therefore provide direct evidence that the amelioration of PD akinesia by DBS is achieved by the disruption of abnormal cortico-basal ganglia oscillations rather than by modulation of the discharge rate.

RESULTS

Experimental Paradigm

The current study was performed on two African green monkeys rendered parkinsonian by systemic application of the neurotoxin MPTP (see Supplemental Information available online; Experimental Procedures). All procedures were conducted in accordance with the Hebrew University guidelines for animal care. We recorded from the GPi and the M1 (n = 127 and 210 neurons, respectively) before, during, and after the application of various stimulation paradigms and examined the effect of stimulation on several outcome parameters. These parameters included the neural oscillatory activity, the pallidal discharge rate and the primates' "kinesis," which is an assessment of their limb movements (Experimental Procedures).

In order to deliver adaptive (i.e., using an algorithm based on ongoing neuronal discharge) stimulation, we constructed an experimental setup in which a copy of the recorded electrodes' analog signal was diverted to a dedicated DSP (Digital Signal Processing) chip (Figure 1A). This allowed initiation of a stimulus

according to an online real-time algorithm based on a signal obtained from any of the recording electrodes. We have termed this group of stimulation paradigms "closed-loop" stimulation paradigms, since they essentially create a feedback loop between the two structures involved (e.g., Figure 1A, bottom panel). This in contrast to nonadaptive systems widely used in the treatment of advanced PD today, in which the stimulus is delivered regardless of the ongoing activity and according to a predefined offline script (Figure 1B).

The paradigm chosen in this study was to deliver a single pulse or a short train (7 pulses at 130 Hz) through a pair of GPi electrodes at a predetermined and fixed latency (80 ms) following the occurrence of an action potential recorded either from the GPi or M1. For each closed-loop stimulation session, two anatomical targets were selected. The first was the reference structure, from whose activity the trigger for stimulation was detected. In this study, the trigger was always a spike in this reference structure, which was either M1 or the GPi. The second was the stimulated structure, to which the stimulus was delivered, in this study always the GPi. In all trials the stimulus was applied through two electrodes located within the GPi, either regardless of the ongoing activity (open-loop paradigms, e.g., standard continuous 130 Hz DBS) or after the identification of a trigger in the ongoing activity (closed-loop paradigms). Throughout this article, we use the following notation: a stimulus consisting of a train of pulses is denoted by the subscript "train"; a stimulus consisting of a single current pulse is denoted by the subscript "sp". The full descriptions of the closed-loop paradigms therefore consist of both the anatomical targets (reference and stimulated structures) and the stimulation pattern, and are expressed as [$STIMULATED_{pattern}$|REFERENCE] (e.g., [GP_{train}|M1], where GPi is the stimulated site and the M1 is the reference site).

Through a number of preliminary experiments, we identified a set of successful parameters for adaptive or closed-loop stimulation paradigms. The stimulation selected was applied 80 ms after detecting a spike in the reference structure. This choice of the delay was made for several reasons. Primarily it made the stimulus coincide with the next double-tremor frequency oscillatory burst (approximately 12.5 Hz), provided the reference spike was a part of a previous burst in the GPi (when the latter was used as reference). In addition, the state of neuronal oscillatory discharge of the cortico-basal ganglia loops is often accompanied by cortico-basal ganglia synchronization (see below). Thus, this delay would also make the stimulus coincide with a GPi oscillatory burst when utilizing the M1 as reference, provided the system was engaged in such pathological synchronization. Furthermore, in the preliminary experiments we tried applying shorter delays, which produced substantially inferior results (Figure 2 and Figure S1). Since the main goal of this work was to compare open- to closed-loop paradigms, we chose to focus on the best closed-loop paradigm found in the preliminary experiments and controlled for it by as many open-loop paradigms as possible. The results of the application of closed-loop stimulation strategies were compared with standard DBS (continuous 130 Hz SP GPi stimulation) and several other control open-loop strategies.

Closed-Loop GP_{train}|M1 DBS Suppresses Pallidal Discharge Rate and Oscillations, While Ameliorating the MPTP-Induced Akinesia

We recorded the activity of 45 GPi neurons before, during and after the application of the GP_{train}|M1 closed-loop stimulus pattern (Figure 1A). The response of a representative pallidal neuron to this stimulation regimen application is shown in Figures 3A–3C. The discharge rate of this neuron showed a dramatic decrease during the GP_{train}|M1 closed-loop stimulation (Figure 3B) compared with the recordings made before (Figure 3A) and after (Figure 3C) the stimulation. In addition to the substantial reduction in discharge rate, the neuron's discharge pattern was also modified and the oscillatory activity was virtually abolished (Figure 3D). The limb akinesia was substantially alleviated, as can be seen from the contralateral limb accelerometer recording trace (Figure 3E). The effect on akinesia was observed in all four limbs of the primate, with the side contralateral to stimulation showing a greater percentage of improvement than the ipsilateral side (Figure S2). The resultant movement mainly exhibited lower frequencies and substantially higher amplitude than the MPTP-induced 4–7 Hz tremor (Figures 5B–5D), confirming that the computed increase in kinesis was not due to an increase in rest tremor. The stimulation pattern, shown in a raster plot (Figure 3E, top trace, and Figure 3F), had a relatively low mean frequency and was highly irregular, containing lengthy epochs during which no stimulus was applied. Both the effects on akinesia (Figure 5A) and on the neuronal discharge (Figures 6B, 7C, and 7D) were statistically significant at the population level as compared with spontaneous recordings during which no stimulation was applied. The effects of the stimulus application on the outcome parameters were reproducible between trials (Figure S3) and there was no apparent accommodation to stimulation over time during the course of the experiments (Figure S4).

Standard (Open-Loop 130 Hz) GPi DBS Reduces Pallidal Oscillations and Akinesia, but to a Lesser Degree Than the GP_{train}|M1 Closed-Loop DBS

In order to compare the effects of the closed-loop stimulation paradigm to the standard GPi DBS regimen (constant 130 Hz single pulse GPi stimulation), we recorded the activity of 47 pallidal neurons before, during and after the application of standard GPi DBS (Figure 1B). The response of a representative pallidal neuron to the application of standard DBS is shown in Figure 4B. When compared with the result of application of the closed-loop GP_{train}|M1 stimulation (Figure 3), this neuron demonstrated only a moderate reduction in its discharge rate. Similarly, the neuron exhibited less pronounced changes in its discharge pattern, which remained bursty and oscillatory during the application of standard DBS (Figure 4D), as previously described (Johnson et al., 2009; McCairn and Turner, 2009). Also in line with previous reports (Boraud et al., 1996; Johnson et al., 2009), the primates' akinesia was alleviated during the application of standard DBS (Figure 4E), albeit to a lesser extent than during the application of GP_{train}|M1 closed-loop stimulation (Figure 3E and Figure S2). Overall, the mean discharge rate of the GPi neurons (Figure 6B) and the M1 and GPi oscillatory activity at the double-tremor frequency band (Figure 7D) were reduced during the application

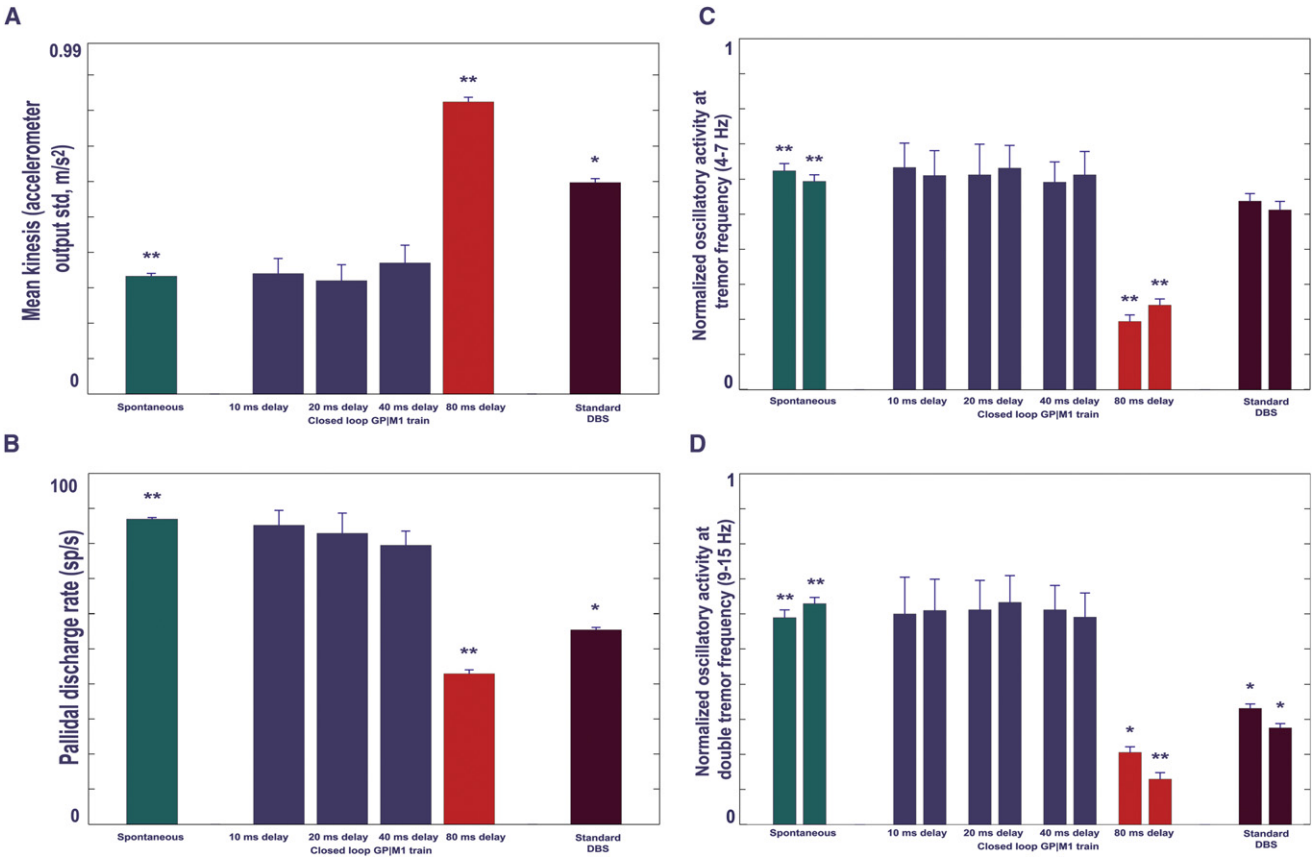

Figure 2. Effect of Delay Manipulation in the Closed-Loop GPtrain|M1 Paradigm on Kinesis and Neural Outcome Parameters

Delay manipulation during the preliminary experiments revealed 80 ms (red bars) superior to other delays (blue bars) and standard continuous 130 Hz DBS (dark red bars) in improving the output parameters by GPtrain|M1 closed-loop DBS.

(A) Kinesis.

(B) Pallidal discharge rate.

(C) tremor frequency oscillatory activity.

(D) Double tremor frequency oscillatory activity.

In (C) and (D): for each stimulation paradigm two columns are shown, one for the M1 activity (left column) and one for the GPi activity (right column); comparisons were made exclusively within structures.

In all panels, n = 2, 3, 3 for the 10, 20, and 40 ms delays, respectively; n = 45 for the 80 ms delay; and n = 47 for standard DBS. The order of columns is spontaneous (green), 10 ms, 20 ms, 40 ms delays (blue), 80 ms delay (red) GPtrain|M1 closed-loop paradigms, standard DBS (dark red). Error bars denote SEM; columns marked *significantly different with $p < 0.05$ compared with all columns marked either * or **; columns marked ** significantly different with $p < 0.01$ compared with all other columns marked ** (one-way ANOVA, Bonferroni adjusted for multiple comparisons).

of standard DBS compared with spontaneous activity, coinciding with an increase in the mean kinesis estimate (Figure 5A). Once again, the effects of stimulus application on the outcome parameters were reproducible between trials (Figure S5).

As expected, the stimulus frequency delivered during the application of $GP_{train}|M1$ closed-loop DBS was significantly lower than that during standard DBS (30.185 ± 2.41 versus 130.007 ± 0.0004 Hz, Figure 1C, one-way ANOVA, $p < 0.01$). Furthermore, stimulus irregularity significantly increased (coefficient of variation of the interstimulus interval duration 5.0605 ± 0.067 versus 0.0003 ± $1.6*10^{-5}$, one-way ANOVA, $p < 0.01$, Figure 1C). However, despite the reduction in the stimulus frequency in the $GP_{train}|M1$ mode, the GPi discharge rate was significantly lower during this closed-loop stimulation than during the standard 130 Hz open-loop GPi DBS (Figure 6B, red versus dark-red bars; one-way ANOVA, $p < 0.05$). When comparing the normalized oscillatory activity at tremor and double-tremor frequencies between the two paradigms, the closed-loop strategy resulted in greater reduction of power in both frequency bands. This was true in both the cortical and the pallidal neuronal populations (one-way ANOVA, $p < 0.01$ for tremor frequency band and $p < 0.05$ for double-tremor frequency band; Figures 7C and 7D, respectively).

Closed-Loop DBS Superiority Is Due to Its Adaptive Nature

We next set out to ensure that the apparent success of the closed-loop stimulation method was indeed due to its adaptive

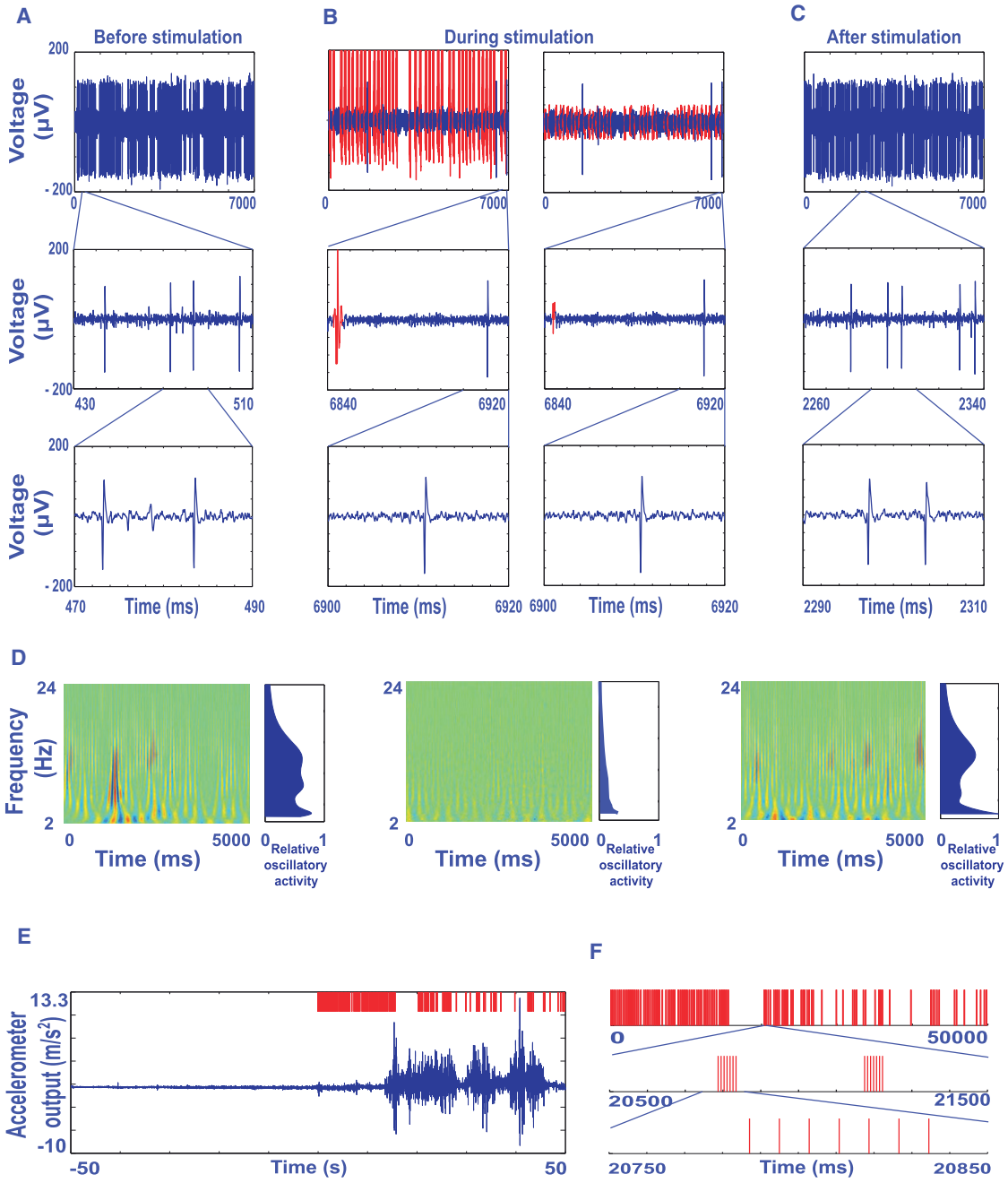

Figure 3. Closed-Loop $GP_{train}|M1$ Stimulation with 80 ms Delay Results in Concurrent Reduction of Pallidal Discharge Rate, Disruption of Pallidal Oscillatory Activity, and Alleviation of Akinesia

(A–C) An example of 7 s analog traces of spiking activity of a GPi neuron before (A), during (B), and after (C) the application of the closed-loop $GP_{train}|M1$ stimulus paradigm (train of seven stimuli delivered to the GPi triggered by M1 spikes, delay = 80 ms). Analog data were filtered between 250 and 5000 Hz (Butterworth 4-pole software filter). The stimulus artifact is shown in red (B, left column), as is the residual artifact after artifact template removal (B, right column). Insets with higher temporal resolution (second and third rows) demonstrate stability of the single-spike waveform throughout the stimulation session and the adjacent spontaneous recordings.

(D) Oscillatory activity depicted through wavelet spectrograms and displayed by frequency as a function of time, with blue to red color indicating the intensity of activity. Spectrograms of activity before (left column), during (middle column), and after (right column) the application of the stimulus paradigm are shown. Power estimates averaged over time (to the right of each spectrogram) are relative to the maximal oscillatory power in the entire recording from this neuron.

(E) Kinesis estimation: 100 s long trace of an analog recording from an accelerometer fastened to the primate's limb contralateral to the stimulating electrodes, 50 s before the onset of stimulation and 50 s during stimulation. Stimulus raster is depicted in red in the upper trace.

(F) Characteristics of the stimulus pattern: a highly irregular stimulus pattern and low stimulus rate.

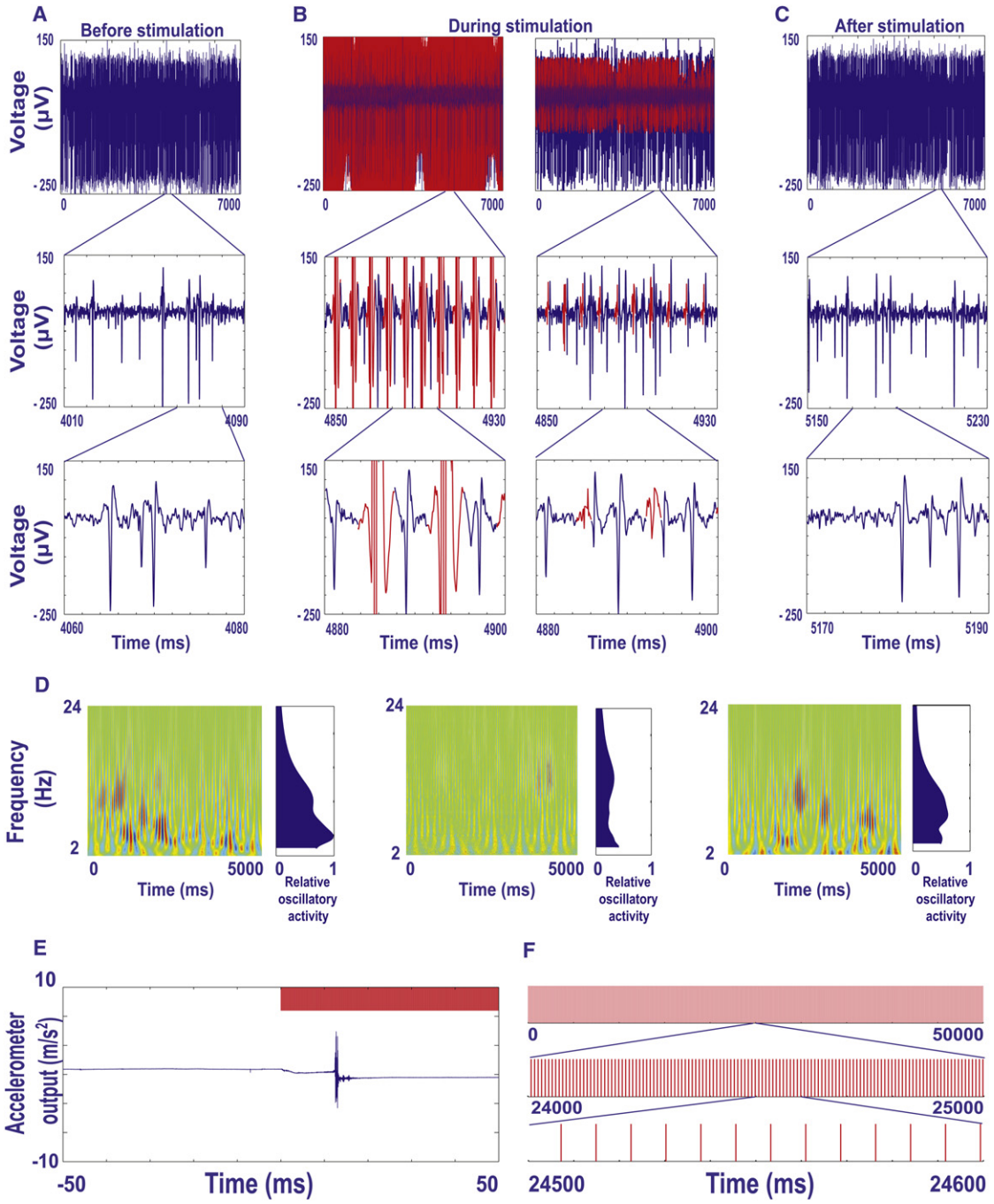

Figure 4. Standard 130 Hz Single Pulse Nonadaptive DBS Only Moderately Affects the Pallidal Discharge Rate, the Pallidal Oscillatory Activity, and the Primates' Akinesia

(A–C) GPi neuron spiking activity before, during, and after the application of standard DBS. Subplot B (left and right column): data before and after stimulus artifact template removal, respectively.

(D) Wavelet spectrogram display of the oscillatory activity.

(E) Kinesis estimation.

(F) Characteristics of the stimulus pattern: a highly regular stimulus pattern with a high stimulus rate of 130 Hz. Same conventions and methods as in Figure 3 apply.

properties. Since setting the stimulus interval to 80 ms from trigger detection could induce a double-tremor frequency rhythm in ongoing activity, we controlled for the effect of application of such a rhythm using open-loop paradigms. We applied GPi nonadaptive 10 Hz stimuli, both in train (seven pulses 130 Hz intratrain frequency) and in single pulse (sp) modes and recorded

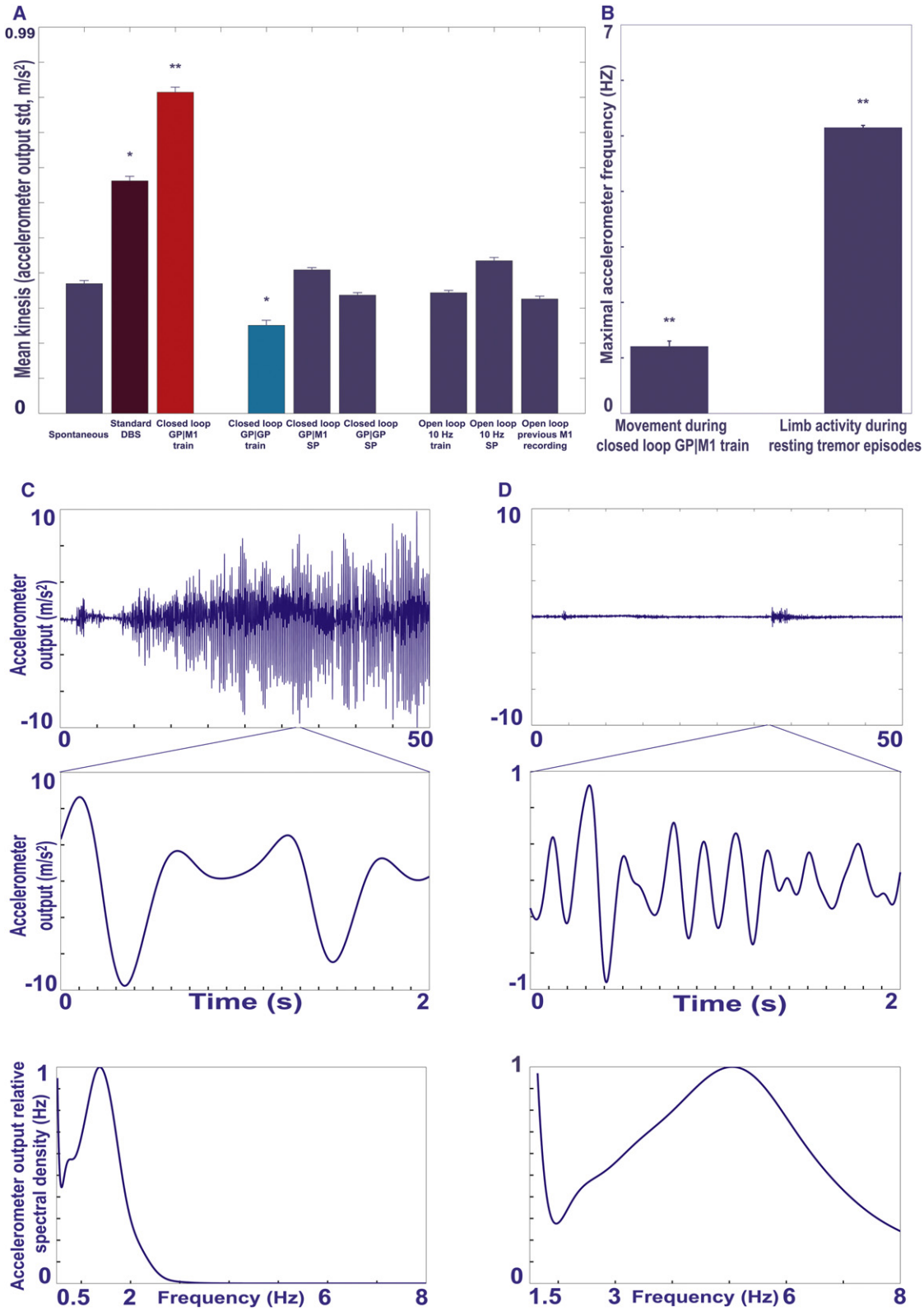

Figure 5. Effects of the Various Stimulation Paradigms on the Primates' Akinesia

(A) Kinesis estimate during the application of different stimulation paradigms and at rest. Kinesis was defined as the average standard deviation of the analog traces recorded from the three movement axes of an accelerometer fastened to a limb contralateral to the stimulation site. Significant differences (as compared

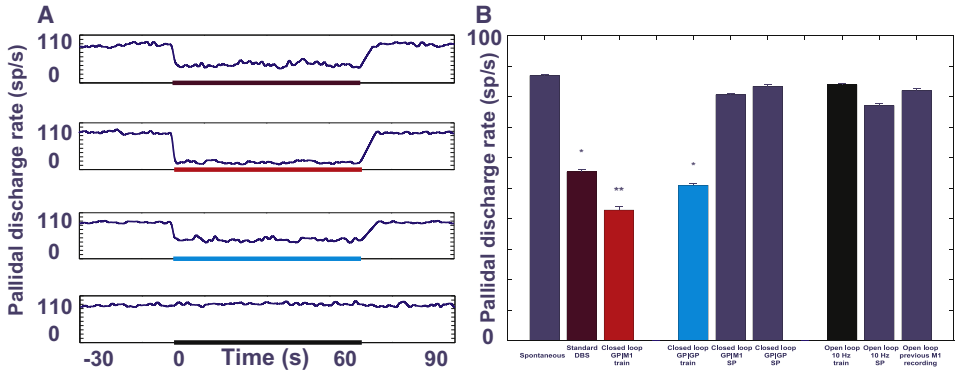

Figure 6. Effects of the Various Stimulation Paradigms on the Pallidal Discharge Rate

Panels in subplot (A) show PSTHs (peri stimulus time histograms, 1 ms bins, smoothed with a Gaussian window, SD 100 ms) of GPi neurons during the application of standard DBS (dark red), closed-loop $GP_{train}|M1$ (red), closed-loop $GP_{train}|GP$ (cyan), and open-loop 10 Hz bursts (black). Stimulation epochs are denoted by a color line on the abscissa, with color matching the appropriate population result in subplot B.

(B) Discharge rate of the entire population of neurons recorded during the application of each stimulation paradigm is given in spikes/s. Results were corrected for the recording dead time of the stimulus artifact. The difference in pallidal firing rate during $GP_{train}|M1$ (red bar) and during standard DBS (dark red bar) application was statistically significant. The GPi discharge rate during the application of the closed-loop $GP_{train}|M1$ (red bar) and $GP_{train}|GP$ (cyan bar) was also significantly different. The only stimulation paradigms yielding a significant difference in GPi discharge rates as compared with spontaneous activity were standard DBS, closed-loop $GP_{train}|GP$ and closed-loop $GP_{train}|M1$. Error bars denote SEM. *Statistically significant difference with $p < 0.05$ compared with all other columns, unless specified otherwise. **Statistically significant difference with $p < 0.01$ compared with all other columns except for those marked with a single asterisk. Comparison performed using one-way ANOVA, Bonferroni adjusted for multiple comparisons.

44 and 35 pallidal neurons during the application of these nonadaptive 10 Hz stimulus paradigms, respectively. The application of these open-loop regimens of stimulation had no apparent effect on the recorded neuronal activity or kinesis (Figures 5–7).

An additional property of the stimulus pattern resulting from the application of the $GP_{train}|M1$ adaptive algorithm was the stimulus pattern's irregularity (Figures 1C and 3F). Recent studies have demonstrated that increasing the stimulus irregularity of open-loop DBS decreases its beneficial clinical effects (Baker et al., 2011; Dorval et al., 2010). Nevertheless, the resultant reduction of firing rate and kinesis improvement achieved by the closed-loop DBS paradigm employed in the current study might still have been due to stimulus irregularity or its resemblance to irregular cortical activity. Had this been the case, it would have obviated the need for the closed-loop architecture of the DBS system. We therefore applied a stimulation pattern based on a previously obtained cortical recording (i.e., unrelated to the ongoing activity during the stimulus application). As expected, the average variability of this stimulus pattern equaled the variability of the $GP_{train}|M1$ closed-loop paradigm (Figure 1C). Nevertheless, the mean discharge rate, the mean kinesis and the oscillatory activity estimates during this paradigm application were not significantly different from those measured during the spontaneous sessions (Figures 5–7).

Pallidal Closed-Loop Paradigm Reveals Dissociation between Discharge Rate and Pattern

An additional result was obtained from other closed-loop paradigms: $GP_{train}|GP$, $GP_{sp}|GP$ and $GP_{sp}|M1$ (n = 52, 41 and 47 pallidal cells, respectively). The latter two paradigms, during which we delivered a single stimulus pulse instead of a train of seven stimuli, did not result in a statistically significant change in any of the examined parameters when compared with spontaneous data (Figures 5–7). However, when examining the $GP_{train}|GP$ results, we found that the pallidal discharge rate was reduced compared with the spontaneous recording (Figure 6, cyan). Unexpectedly, the kinesis estimate was also reduced (i.e., the primate's akinesia worsened, Figure 5). The remarkable worsening of akinesia despite the reduction of GPi discharge rate might be due a significant enhancement of cortical oscillatory activity at double-tremor frequency (Figure 7D,

with spontaneous movement) were observed during the application of standard DBS (dark red bar), closed-loop $GP_{train}|M1$ (red bar) and closed-loop $GP_{train}|GP$ (cyan bar).

(B) Spectral analysis of the arm's voluntary and involuntary movements: for each trial the frequency of the maximal value of the limb movement spectral density function was measured. Population results are shown during the application of closed-loop $GP_{train}|M1$ stimulus (left column) and during spontaneous rest tremor (right column), forty 50 s long segments in each group. In subplots A and B: error bars denote SEM. *Statistically significant difference with $p < 0.05$ compared with all other columns. **Statistically significant difference with $p < 0.01$ compared with all other columns except for those marked with a single asterisk. All comparisons were performed using one-way ANOVA; Bonferroni was adjusted for multiple comparisons where appropriate.

(C and D) Two 50 s long traces of accelerometer recordings from the arm contralateral to the stimulating electrodes, during $GP_{train}|M1$ stimulus application (C) and during a spontaneous recording containing tremor episodes (D), are shown in the upper row panels. Two second long insets in middle row panels of (C) and (D) show the different temporal properties of the accelerometer traces (note different Y-scales of insets). Bottom row panels indicate the power spectra of the traces depicted in the top row, each relative to the maximal power of the frequency range examined.

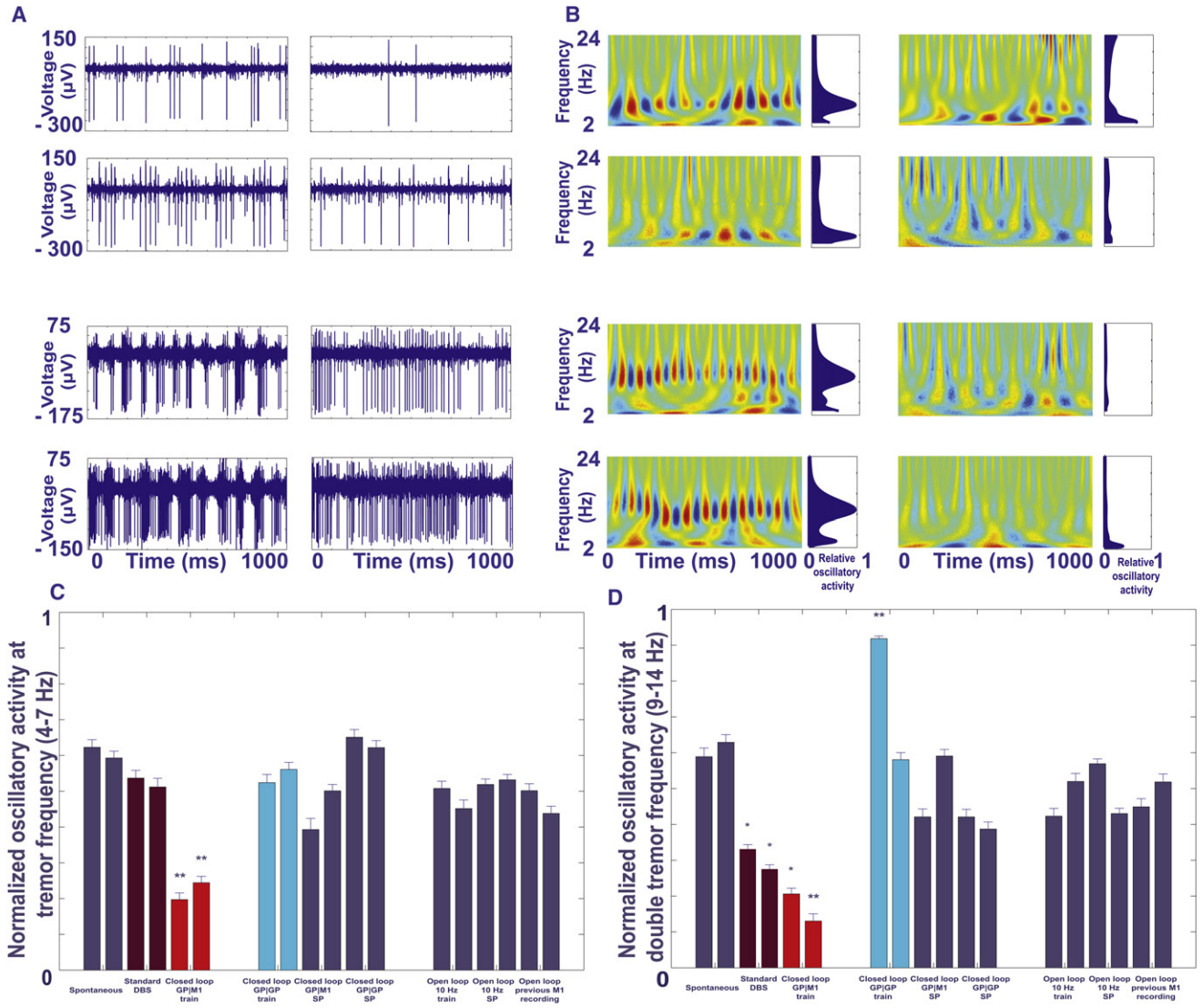

Figure 7. Effects of the Various Stimulation Paradigms on the Ongoing Oscillatory Discharge in the M1 and the GPi

Subplots A and B demonstrate the intermittent nature of the oscillatory activity in the M1 and the GPi of the primate MPTP model of PD.

(A) An analog trace of four electrode recordings (250–5000 Hz band-pass filtered) from the M1 (top two panels) and the GPi (bottom two panels) during a period of neuronal oscillations (left column) and during cessation of this activity (right column). The electrode in second trace from the top (located in M1) demonstrated oscillatory activity at tremor frequency range (4–7 Hz), whereas the other electrodes demonstrated oscillatory activity at double-tremor frequency range (9–14 Hz).

(B) Wavelet spectrograms of activity depicted in the analog traces in subplot A. Spectrograms are displayed by frequency (y axis) as a function of time (x axis), with color ranging from blue to red; coding for low to high intensity of activity. The oscillatory power estimates averaged over time were computed relative to the maximal oscillatory activity in each particular recording and are shown to the right of each spectrogram. Subplots C and D summarize the population results.

(C) Oscillatory activity in the tremor frequency range (4–7 Hz). For each stimulation paradigm two columns are shown, one for the M1 activity (left column) and one for the GPi activity (right column). Comparisons were made exclusively within structures (i.e., cortical activity compared only to cortical activity and GPi activity compared with GPi activity).

(D) Normalized oscillatory activity in the double-tremor frequency range (9–14 Hz). Same conventions as in subplot C apply.

Error bars in (C) and (D) denote SEM.

cyan). These differences were statistically significant at the population level ($p < 0.05$ and $p < 0.01$, respectively, one-way ANOVA, Figures 5–7), demonstrating a clear dissociation between discharge rate and discharge pattern in the cortex-basal ganglia network.

DISCUSSION

In this study, we derive a novel real-time adaptive method for treatment of brain disorders characterized by a recognizable pathological pattern of neural activity. This type of stimulation

in essence creates a feedback loop between two neuronal structures, using the trigger detected in the reference structure as the feedback loop input and delivering the feedback loop output to the stimulated structure (Figure 1A). We have therefore termed such stimulation "closed-loop" stimulation. We demonstrate that in the MPTP-treated primate, closed-loop stimulation of the GPi based on the ongoing activity in M1 is more efficient in alleviating parkinsonian motor symptoms than the standard continuous (open-loop) high-frequency GPi DBS paradigm. Furthermore, closed-loop DBS is also accompanied by a greater reduction in oscillatory activity in both the pallidum and the primary motor cortex as compared with standard DBS. The current study could therefore serve as a "proof of concept" for the utilization of closed-loop stimulation paradigms in the treatment of brain disorders in general and PD in particular. In addition, our results suggest that the role of the oscillatory activity of cortico-basal ganglia loops is more significant than that of the changes in their discharge rate with regards to the generation of akinesia, the main motor symptom of Parkinson's disease. Thus, this study also provides an insight into the underlying pathophysiology of PD and indications for the future directions of closed-loop DBS research and utilization.

Discharge Rates versus Discharge Patterns in the Cortico-Basal Ganglia Networks

Previous models of the corticobasal ganglia networks have emphasized the role of changes in discharge rate of the BG neurons in the generation of PD symptoms (Albin et al., 1989; Bergman et al., 1990), a view that is now considered to be incomplete (Hammond et al., 2007; Wichmann and DeLong, 2006). Indeed, the application of both the standard DBS and $GP_{train}|M1$ closed-loop stimulation resulted in improvement of the primates' motor deficits (Figure 5A), which coincided with a reduction in the pallidal discharge rate (Figure 6B). However, this improvement also coincided with a reduction in oscillatory activity (Figures 7C and 7D). While the reduction in oscillatory activity was limited to double-tremor frequency oscillations during standard DBS application, it also occurred at tremor frequency in the closed-loop $GP_{train}|M1$ paradigm. Furthermore, the reduction in GPi double-tremor frequency oscillatory activity was more pronounced during the application of the $GP_{train}|M1$ paradigm (Figure 7D). Notably, the pallidal oscillatory activity was not correlated to the pallidal discharge rate either before or during the application of standard DBS and closed-loop $GP_{train}|M1$, which is suggestive of independent mechanisms behind the two phenomena (Figures S6 and S7). These results are in line with a recent report indicating that independent mechanisms may underlie the burst discharges and oscillatory activity of most GPi neurons in human PD patients (Chan et al., 2011). These findings therefore suggest, in agreement with other recent studies (Eusebio and Brown, 2007; Hammond et al., 2007; Kühn et al., 2009; Tass et al., 2010; Vitek, 2008; Weinberger et al., 2009; Wichmann and DeLong, 2006; Zaidel et al., 2009), that changes in discharge patterns, in particular, changes in the oscillatory activity of the parkinsonian cortico-basal ganglia loops, are at least equally likely to play a key role in PD pathophysiology as are changes in the pallidal discharge rate.

The above suggestion was strongly reinforced by the results of $GP_{train}|GP$ closed-loop application (GPi short train stimulation 80 ms following the detection of a GPi spike). The dissociation between the reduction in the GPi discharge rate versus the insignificant effect on the GPi oscillations and even an increase in M1 double-tremor oscillatory activity was actually accompanied by worsening of the akinesia. This indicates that changes in discharge patterns may in fact be more crucial than changes in discharge rates for the development of the clinical symptoms of PD. The fact that the modulation of oscillatory activity coincided in both magnitude and direction with the changes of parkinsonian motor symptoms during both open and closed-loop DBS sessions constitutes a strong argument in favor of the detrimental role of these oscillations in PD pathophysiology. Equally important, it suggests that reduction of the abnormal parkinsonian oscillatory activity could in fact be the underlying mechanism by which DBS exerts its action and brings about the associated clinical improvement. Furthermore, we found a significant correlation between pallidal oscillatory activity before the application of both standard DBS and closed-loop $GP_{train}|M1$ and the improvement in akinesia achieved during stimulation. This contrasted with the pallidal discharge rate prior to stimulation, which displayed no significant correlation with the improvement in akinesia brought about by either type of stimulation (Figure 8).

Possible Mechanisms of Closed-Loop DBS

When attempting to propose a pathophysiological mechanism behind the superiority of closed-loop over open-loop paradigms, one must take into account the various discharge patterns occurring within the parkinsonian corticobasal ganglia loops. Of special interest are patterns absent from normal brain activity, such as the transient neuronal oscillatory activity within the loops (Figure 7) and neuronal synchronization between loop components. Studies on the dynamics of the entire cortico-basal ganglia loops have frequently reported the emergence of intra- and interloop component synchrony and oscillatory activity (Brown, 2003; Cassim et al., 2002; Eusebio and Brown, 2009; Goldberg et al., 2002, 2004; Hammond et al., 2007; Heimer et al., 2002; Mallet et al., 2008; Raz et al., 1996, 2000; Weinberger et al., 2009). Furthermore, it has been suggested that synchronized neuronal oscillatory activity in the pallidum and the cortex is related to the motor deficits of parkinsonism (Levy et al., 2002; Timmermann et al., 2003). The nature of the coherence between the two structures was shown to be dynamic and state dependent (Lalo et al., 2008; Magill et al., 2004).

Nevertheless, the somewhat intuitive connection between neuronal oscillations and parkinsonian motor symptoms, which include rest and action tremors, has been challenged (Hammond et al., 2007; Leblois et al., 2007; Lozano and Eltahawy, 2004; Tass et al., 2010; Vitek, 2002; Weinberger et al., 2009). For instance, while the parkinsonian rest tremor occurs mainly at the 4–7 Hz frequency band, the oscillatory neuronal activity is observed in several characteristic frequency bands in both human PD patients (Hutchison et al., 2004) and animal models (Bergman et al., 1994; Gubellini et al., 2009). Our study provides strong support for the pathological role of these oscillations, in that stimulation targeted directly at this activity (in a specific band,

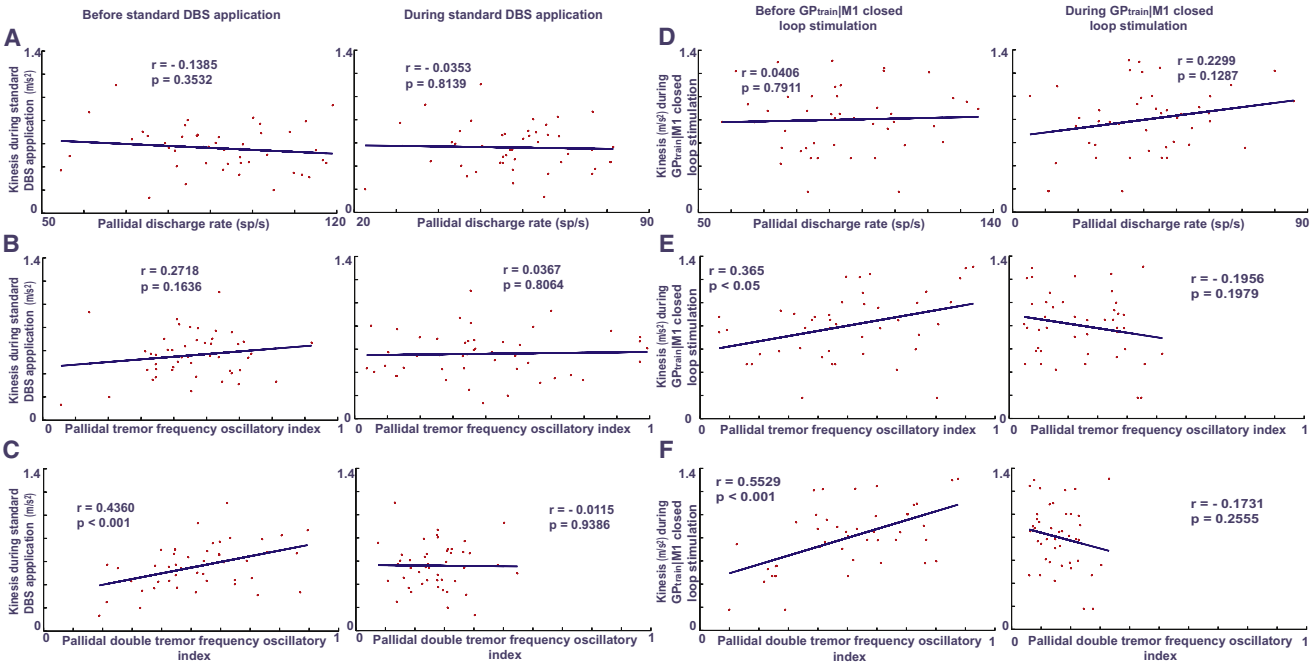

Figure 8. Clinical Improvement during the Application of Standard DBS and Closed-Loop $GP_{train}|M1$ Is Significantly Correlated with Pallidal Double-Tremor Frequency Oscillatory Activity before Stimulus Application, but Not with Pallidal Discharge Rate

The effect of pallidal discharge rate and oscillatory activity before (left column) and during (right column) the application of standard DBS (A–C) and closed-loop $GP_{train}|M1$ (D–F) on the primates' kinesis. Effect examined by computing the correlation coefficient between the parameter in question and kinesis.

(A and D) Discharge rate.

(B and E) Tremor frequency oscillatory index.

(C and F) Double-tremor frequency oscillatory index.

For all panels: r, correlation coefficient; p, p value; line, linear regression. n = 47 for standard DBS and n = 45 for closed-loop $GP_{train}|M1$.

the double-tremor frequency band, approximately 9–15 Hz) provided greater alleviation of parkinsonian motor symptoms than standard DBS.

The fact that M1-based closed-loop stimulation was the most successful in improving all the output parameters is perhaps not too surprising considering the central role of cortical discharge patterns in the pathophysiology of PD. M1 is one of the main components of the cortico-basal ganglia loops, and although the GPi (and the SNr) are the main output nuclei of the basal ganglia network, the M1 is the main output via the corticospinal and corticobrainstem tracts (Albin et al., 1989; Alexander et al., 1986; Alexander and Crutcher, 1990; Bergman et al., 1990; Mink, 1996). Furthermore, M1's direct projection to the STN (Nambu et al., 2000) makes it a perfect candidate to serve as a reference structure in future closed-loop stimulation of the STN. The M1 has been implicated in many aspects of parkinsonian brain activity, such as oscillatory discharge and transient synchronization with pallidal activity (Cassim et al., 2002; Goldberg et al., 2002). Such synchronization during epochs of double-tremor frequency oscillatory discharge could be the basis for the success of $GP_{train}|M1$ when using 80 ms delays compared with the apparent ineffectiveness of other delays, as indicated by our preliminary studies (Figure 2 and Figure S1). A stimulus delivered to the GPi during an oscillatory burst synchronized to its double-tremor frequency counterpart in M1 would disrupt this pathological activity of the pallidum and via the thalamus in M1 itself. On the other hand, when no such synchronization exists, the effect of $GP_{train}|M1$ stimulation on the pallidal discharge would be less significant. Since GP stimulation could, in fact, activate efferent GPi axons while inhibiting their somata (Johnson and McIntyre, 2008), this mechanism could also explain the worsening of akinesia during $GP_{train}|GP$ application. Such activation of GPi efferent axons could in essence induce double-tremor frequency oscillations during $GP_{train}|GP$ stimulation by activating GPi targets 80 ms after a previous GPi spike/burst, even if the latter was originally independent of oscillatory activity.

Most current models of the BG network assume competitive dynamic (Frank et al., 2007; Mink, 1996) and even active decorrelations (Bar-Gad et al., 2000; Parush et al., 2011) of the BG activity. Therefore, these models predict inferior information processing of the BG network upon the emergence of synchronized activity that disrupts these decorrelations. Furthermore, large-scale synchronization of cortical activity could serve as the basis for akinesia (Brown, 2006). Since synchronization and oscillations tend to coincide, manipulations affecting one can affect the other and therefore the closed-loop stimulation in this study could disrupt synchrony as well. However, previous studies have demonstrated that oscillations and synchrony can exist independently (Heimer et al., 2006). Since theoretical studies have demonstrated the plausibility of closed-loop systems targeted at synchronization of activity

(Popovych et al., 2005; Tass, 2003), further experimental studies are needed.

Closed-Loop Deep Brain Stimulation: Limitations and Future Directions

The closed-loop approach suggested in this study may not be limited to PD. Work done on animal models of several neurological and psychiatric disorders indicate that recognizable pathological patterns emerge (Uhlhaas and Singer, 2006). Some bear marked resemblance to the patterns seen in PD; namely, synchrony and oscillatory activity are seen in schizophrenia, a highly prevalent and extremely debilitating psychiatric disorder (Uhlhaas and Singer, 2010). Attempts at using closed-loop approaches for the treatment of other brain disorders will first need to be made in animal models, where the study of the MPTP primate model substantially facilitates the investigation of PD (Langston et al., 1984; Redmond et al., 1985).

We did not carry out a comprehensive investigation to determine the optimal parameters for closing the DBS loop. The aggravation of akinesia during the closed-loop $GP_{train}|GP$ stimulus application (with 80 ms delay) may be due to the positive feedback to the ongoing oscillatory activity in the GPi, and further manipulation of the stimulus delay might identify the working regimens for a GPi based feedback paradigm. Using the same location for both reference and stimulation would no doubt reduce the surgical complexity (Rouse et al., 2011). Moreover, since the neuronal oscillatory activity demonstrated in PD patients includes higher frequencies (beta band, approximately 15–35 Hz) than those observed in MPTP-treated primates, a delay that will best fit these frequencies should be chosen when attempting closed-loop stimulation in human PD patients (de Solages et al., 2010; Eusebio and Brown, 2009; Hammond et al., 2007; Kühn et al., 2009; Mallet et al., 2008; Weinberger et al., 2009; Zaidel et al., 2009). Further studies should be performed to ensure the safety and maximal efficacy of different closed-loop parameters in experimental models of PD and human PD patients. These studies should examine the effects of changing the neural location used as the stimulation reference and the stimulated location (e.g., GPi versus STN; Follett et al., 2010; Moro et al., 2010). In addition, the spatial shape of the stimulation field should be manipulated (McIntyre et al., 2009; Mikos et al., 2011). Since single-unit recordings tend to be unstable over time, the neural signals employed for trigger determination should also be varied (local field potentials, multiunit activity, spike or burst detection). In particular, local field potentials in the parkinsonian brain have been shown to synchronize with the spiking activity in the pallidum (Goldberg et al., 2004; Moran and Bar-Gad, 2010) and thus seem an excellent candidate for future systems employed over long periods of time (Figure S8). Finally, the impact of dopamine replacement therapy (e.g., l-DOPA) on the effects of closed-loop DBS should be examined, as virtually all advanced PD patients are treated with various regimens of dopamine replacement therapy in parallel to DBS.

CONCLUDING REMARKS

In this article, we demonstrate that parkinsonian corticobasal ganglia loops display observability and controllability properties (Lathi, 2004; Nise, 2007) and can therefore be modulated by closed-loop stimulation strategies. Such strategies proved superior to standard DBS in both alleviating the main motor symptom of experimental parkinsonism and disrupting the oscillatory discharge patterns of the parkinsonian cortico-basal ganglia loops. It is therefore our hope that in the near future we will see a new era of DBS strategies, based on various closed-loop paradigms targeted at different pathological aspects of brain activity (Batista et al., 2010; Feng et al., 2007; Stanslaski et al., 2009; Tass, 2003). Such strategies have potential not only for the treatment of PD, but perhaps of other neurological disorders in which a clear pathological pattern of brain activity can be recognized (Uhlhaas and Singer, 2006).

EXPERIMENTAL PROCEDURES

Animals

The experiments were performed on two African green monkeys (Cercopithecus aethiops aethiops), rendered parkinsonian by the systemic application of the neurotoxin MPTP (Supplemental Information). All procedures were conducted in accordance with the Hebrew University guidelines for animal care and the National Institute of Health Guide for the Care and Use of Laboratory Animals.

Neuronal Data

We recorded 127 pallidal and 210 cortical neurons combined during the application of all stimulation types. Only neurons that were judged by the experimenters to be correctly located within the above structures, using the methods described in Supplemental Experimental Procedures, Data Collection, were used in this study. Neurons were considered for acquisition only if they demonstrated stability of the action potential waveform, discharge rate and a consistent refractory period during spontaneous recordings (Hill et al., 2011).

Real-Time Closed-Loop Stimulation

We constructed a custom real-time stimulator capable of delivering current stimuli based on a predefined trigger occurring in ongoing brain activity. A complete description of the stimulation paradigms employed in this study is given in the introduction. All pulses were cathodic-anodic biphasic square current pulses, with the total amplitude of current delivered through the two microelectrodes in each pulse equal to 80 μA and each phase duration equal to 200 μs. The stimulation was delivered 80 ms after the identification of the trigger. Further spikes detected within this 80 ms time offset and the train/stimulus delivery time were ignored. Because of the time constraints in primate MPTP studies and the apparent success of the 80 ms delays, we did not pursue other delays further and the amount of existing data for $\neq$ 80 ms delays is insufficient for a robust statistical analysis (Figure 2).

Outcome Parameters and Analysis

We assessed the results of the various paradigms by estimating their effect on several outcome parameters: neural oscillatory activity, the pallidal discharge rate and an assessment of the primates' limb movements, "kinesis." The latter was estimated using accelerometers fastened to the limbs of the primates. Pooled data are presented as mean ± SEM. Comparisons performed using one-way ANOVA, Bonferroni adjusted for multiple comparisons where appropriate.

A detailed description of all experimental procedures is provided in the Supplemental Information.

SUPPLEMENTAL INFORMATION

Supplemental Information includes Supplemental Experimental Procedures and eight figures and can be found with this article online at doi:10.1016/j.neuron.2011.08.023.

ACKNOWLEDGMENTS

We thank Abraham Solomon (Department of Ophthalmology, Hadassah University Hospital, Jerusalem, Israel), Genela Morris (Department of Neurobiology, University of Haifa, Israel), Ahmed Moustafa (Center for Molecular and Behavioral Neuroscience, Rutgers University, NJ), Harry Xenias (Center for Molecular and Behavioral Neuroscience, Rutgers University, NJ), Eden Chlamtac (School of Computer Science, Tel Aviv University, Israel), and Timothy Denison (Medtronic Technology, MN) for reviewing early versions of this manuscript; Mati Joshua (Department of Clinical Neurobiology, The Hebrew University School of Medicine, Jerusalem, Israel) for suggestions in experimental design; Alpha-Omega Engineering (Nazareth, Israel) for providing the DSP used in the experiments; Tuvia Kurz for the primate illustrations in Figure 1; and Esther Singer for English editing. This study was supported by the Netherlands friends of the Hebrew University (HUNA) "Fighting against Parkinson," the Vorst family, and Dekker foundation grants. Authors' contributions: B.R. assembled the experimental setup and wrote the necessary software; B.R. and H.B. designed the experimental paradigm; E.V. performed the primate surgeries, together with M.R.-E (first primate) and Z.I. (second primate); H.B. and B.R. served as anesthesiologist and an assistant in the surgeries, respectively; B.R., M.S., R.M., and M.R.-E performed the experiments; S.N.H. performed the histological analysis; and B.R. and H.B. conducted the analysis and wrote the manuscript. All authors discussed the results, reviewed the manuscript, and made their comments.

Accepted: August 29, 2011
Published: October 19, 2011

REFERENCES

Albin, R.L., Young, A.B., and Penney, J.B. (1989). The functional anatomy of basal ganglia disorders. Trends Neurosci. *12*, 366–375.

Alexander, G.E., and Crutcher, M.D. (1990). Functional architecture of basal ganglia circuits: neural substrates of parallel processing. Trends Neurosci. *13*, 266–271.

Alexander, G.E., DeLong, M.R., and Strick, P.L. (1986). Parallel organization of functionally segregated circuits linking basal ganglia and cortex. Annu. Rev. Neurosci. *9*, 357–381.

Baker, K.B., Zhang, J., and Vitek, J.L. (2011). Pallidal stimulation: Effect of pattern and rate on bradykinesia in the non-human primate model of Parkinson's disease. Exp. Neurol. *231*, 309–313.

Bar-Gad, I., Havazelet-Heimer, G., Goldberg, J.A., Ruppin, E., and Bergman, H. (2000). Reinforcement-driven dimensionality reduction—a model for information processing in the basal ganglia. J. Basic Clin. Physiol. Pharmacol. *11*, 305–320.

Bar-Gad, I., Elias, S., Vaadia, E., and Bergman, H. (2004). Complex locking rather than complete cessation of neuronal activity in the globus pallidus of a 1-methyl-4-phenyl-1,2,3,6-tetrahydropyridine-treated primate in response to pallidal microstimulation. J. Neurosci. *24*, 7410–7419.

Batista, C.A., Lopes, S.R., Viana, R.L., and Batista, A.M. (2010). Delayed feedback control of bursting synchronization in a scale-free neuronal network. Neural Netw. *23*, 114–124.

Benabid, A.L., Chabardes, S., Torres, N., Piallat, B., Krack, P., Fraix, V., and Pollak, P. (2009). Functional neurosurgery for movement disorders: a historical perspective. Prog. Brain Res. *175*, 379–391.

Bergman, H., Wichmann, T., and DeLong, M.R. (1990). Reversal of experimental parkinsonism by lesions of the subthalamic nucleus. Science *249*, 1436–1438.

Bergman, H., Wichmann, T., Karmon, B., and DeLong, M.R. (1994). The primate subthalamic nucleus. II. Neuronal activity in the MPTP model of parkinsonism. J. Neurophysiol. *72*, 507–520.

Boraud, T., Bezard, E., Bioulac, B., and Gross, C. (1996). High frequency stimulation of the internal Globus Pallidus (GPi) simultaneously improves parkinsonian symptoms and reduces the firing frequency of GPi neurons in the MPTP-treated monkey. Neurosci. Lett. *215*, 17–20.

Bronstein, J.M., Tagliati, M., Alterman, R.L., Lozano, A.M., Volkmann, J., Stefani, A., Horak, F.B., Okun, M.S., Foote, K.D., Krack, P., et al. (2011). Deep brain stimulation for Parkinson disease: an expert consensus and review of key issues. Arch. Neurol. *68*, 165.

Brown, P. (2003). Oscillatory nature of human basal ganglia activity: relationship to the pathophysiology of Parkinson's disease. Mov. Disord. *18*, 357–363.

Brown, P. (2006). Bad oscillations in Parkinson's disease. J. Neural Transm. Suppl. 27–30.

Carlson, J.D., Cleary, D.R., Cetas, J.S., Heinricher, M.M., and Burchiel, K.J. (2010). Deep brain stimulation does not silence neurons in subthalamic nucleus in Parkinson's patients. J. Neurophysiol. *103*, 962–967.

Cassim, F., Labyt, E., Devos, D., Defebvre, L., Destée, A., and Derambure, P. (2002). Relationship between oscillations in the basal ganglia and synchronization of cortical activity. Epileptic Disord. *4* (*Suppl 3*), S31–S45.

Chan, V., Starr, P.A., and Turner, R.S. (2011). Bursts and oscillations as independent properties of neural activity in the parkinsonian globus pallidus internus. Neurobiol. Dis. *41*, 2–10.

de Solages, C., Hill, B.C., Koop, M.M., Henderson, J.M., and Bronte-Stewart, H. (2010). Bilateral symmetry and coherence of subthalamic nuclei beta band activity in Parkinson's disease. Exp. Neurol. *221*, 260–266.

Deniau, J.M., Degos, B., Bosch, C., and Maurice, N. (2010). Deep brain stimulation mechanisms: beyond the concept of local functional inhibition. Eur. J. Neurosci. *32*, 1080–1091.

Deuschl, G., Herzog, J., Kleiner-Fisman, G., Kubu, C., Lozano, A.M., Lyons, K.E., Rodriguez-Oroz, M.C., Tamma, F., Tröster, A.I., Vitek, J.L., et al. (2006). Deep brain stimulation: postoperative issues. Mov. Disord. *21* (*Suppl 14*), S219–S237.

Dorval, A.D., Kuncel, A.M., Birdno, M.J., Turner, D.A., and Grill, W.M. (2010). Deep brain stimulation alleviates parkinsonian bradykinesia by regularizing pallidal activity. J. Neurophysiol. *104*, 911–921.

Dostrovsky, J.O., Levy, R., Wu, J.P., Hutchison, W.D., Tasker, R.R., and Lozano, A.M. (2000). Microstimulation-induced inhibition of neuronal firing in human globus pallidus. J. Neurophysiol. *84*, 570–574.

Eusebio, A., and Brown, P. (2007). Oscillatory activity in the basal ganglia. Parkinsonism Relat. Disord. *13* (*Suppl 3*), S434–S436.

Eusebio, A., and Brown, P. (2009). Synchronisation in the beta frequency-band—the bad boy of parkinsonism or an innocent bystander? Exp. Neurol. *217*, 1–3.

Feng, X.J., Greenwald, B., Rabitz, H., Shea-Brown, E., and Kosut, R. (2007). Toward closed-loop optimization of deep brain stimulation for Parkinson's disease: concepts and lessons from a computational model. J. Neural Eng. *4*, L14–L21.

Follett, K.A., Weaver, F.M., Stern, M., Hur, K., Harris, C.L., Luo, P., Marks, W.J., Jr., Rothlind, J., Sagher, O., Moy, C., et al; CSP 468 Study Group. (2010). Pallidal versus subthalamic deep-brain stimulation for Parkinson's disease. N. Engl. J. Med. *362*, 2077–2091.

Frank, M.J., Samanta, J., Moustafa, A.A., and Sherman, S.J. (2007). Hold your horses: impulsivity, deep brain stimulation, and medication in parkinsonism. Science *318*, 1309–1312.

Frankemolle, A.M., Wu, J., Noecker, A.M., Voelcker-Rehage, C., Ho, J.C., Vitek, J.L., McIntyre, C.C., and Alberts, J.L. (2010). Reversing cognitive-motor impairments in Parkinson's disease patients using a computational modelling approach to deep brain stimulation programming. Brain *133*, 746–761.

Goldberg, J.A., Boraud, T., Maraton, S., Haber, S.N., Vaadia, E., and Bergman, H. (2002). Enhanced synchrony among primary motor cortex neurons in the 1-methyl-4-phenyl-1,2,3,6-tetrahydropyridine primate model of Parkinson's disease. J. Neurosci. *22*, 4639–4653.

Goldberg, J.A., Rokni, U., Boraud, T., Vaadia, E., and Bergman, H. (2004). Spike synchronization in the cortex/basal-ganglia networks of Parkinsonian primates reflects global dynamics of the local field potentials. J. Neurosci. *24*, 6003–6010.

Gubellini, P., Salin, P., Kerkerian-Le Goff, L., and Baunez, C. (2009). Deep brain stimulation in neurological diseases and experimental models: from molecule to complex behavior. Prog. Neurobiol. *89*, 79–123.

Hammond, C., Bergman, H., and Brown, P. (2007). Pathological synchronization in Parkinson's disease: networks, models and treatments. Trends Neurosci. *30*, 357–364.

Heimer, G., Bar-Gad, I., Goldberg, J.A., and Bergman, H. (2002). Dopamine replacement therapy reverses abnormal synchronization of pallidal neurons in the 1-methyl-4-phenyl-1,2,3,6-tetrahydropyridine primate model of parkinsonism. J. Neurosci. *22*, 7850–7855.

Heimer, G., Rivlin, M., Israel, Z., and Bergman, H. (2006). Synchronizing activity of basal ganglia and pathophysiology of Parkinson's disease. J. Neural Transm. Suppl. 17–20.

Hill, D.N., Mehta, S.B., and Kleinfeld, D. (2011). Quality metrics to accompany spike sorting of extracellular signals. J. Neurosci. *31*, 8699–8705.

Hurtado, J.M., Rubchinsky, L.L., Sigvardt, K.A., Wheelock, V.L., and Pappas, C.T. (2005). Temporal evolution of oscillations and synchrony in GPi/muscle pairs in Parkinson's disease. J. Neurophysiol. *93*, 1569–1584.

Hutchison, W.D., Dostrovsky, J.O., Walters, J.R., Courtemanche, R., Boraud, T., Goldberg, J., and Brown, P. (2004). Neuronal oscillations in the basal ganglia and movement disorders: evidence from whole animal and human recordings. J. Neurosci. *24*, 9240–9243.

Johnson, M.D., and McIntyre, C.C. (2008). Quantifying the neural elements activated and inhibited by globus pallidus deep brain stimulation. J. Neurophysiol. *100*, 2549–2563.

Johnson, M.D., Vitek, J.L., and McIntyre, C.C. (2009). Pallidal stimulation that improves parkinsonian motor symptoms also modulates neuronal firing patterns in primary motor cortex in the MPTP-treated monkey. Exp. Neurol. *219*, 359–362.

Kühn, A.A., Tsui, A., Aziz, T., Ray, N., Brücke, C., Kupsch, A., Schneider, G.H., and Brown, P. (2009). Pathological synchronisation in the subthalamic nucleus of patients with Parkinson's disease relates to both bradykinesia and rigidity. Exp. Neurol. *215*, 380–387.

Lafreniere-Roula, M., Kim, E., Hutchison, W.D., Lozano, A.M., Hodaie, M., and Dostrovsky, J.O. (2010). High-frequency microstimulation in human globus pallidus and substantia nigra. Exp. Brain Res. *205*, 251–261.

Lalo, E., Thobois, S., Sharott, A., Polo, G., Mertens, P., Pogosyan, A., and Brown, P. (2008). Patterns of bidirectional communication between cortex and basal ganglia during movement in patients with Parkinson disease. J. Neurosci. *28*, 3008–3016.

Langston, J.W., Irwin, I., and Langston, E.B. (1984). A comparison of the acute and chronic effects of 1-methyl-4-phenyl-1,2,5,6-tetrahydropyridine (MPTP)-induced parkinsonism in humans and the squirrel monkey. Neurology *34* (*Suppl. 1*), 268.

Lathi, B.P. (2004). Linear Systems and Signals (New York: Oxford University Press).

Leblois, A., Meissner, W., Bioulac, B., Gross, C.E., Hansel, D., and Boraud, T. (2007). Late emergence of synchronized oscillatory activity in the pallidum during progressive Parkinsonism. Eur. J. Neurosci. *26*, 1701–1713.

Lee, J.Y., Jeon, B.S., Paek, S.H., Lim, Y.H., Kim, M.R., and Kim, C. (2010). Reprogramming guided by the fused images of MRI and CT in subthalamic nucleus stimulation in Parkinson disease. Clin. Neurol. Neurosurg. *112*, 47–53.

Levy, R., Hutchison, W.D., Lozano, A.M., and Dostrovsky, J.O. (2002). Synchronized neuronal discharge in the basal ganglia of parkinsonian patients is limited to oscillatory activity. J. Neurosci. *22*, 2855–2861.

Lozano, A.M., and Eltahawy, H. (2004). How does DBS work? Suppl. Clin. Neurophysiol. *57*, 733–736.

Magill, P.J., Sharott, A., Bolam, J.P., and Brown, P. (2004). Brain state-dependency of coherent oscillatory activity in the cerebral cortex and basal ganglia of the rat. J. Neurophysiol. *92*, 2122–2136.

Mallet, N., Pogosyan, A., Sharott, A., Csicsvari, J., Bolam, J.P., Brown, P., and Magill, P.J. (2008). Disrupted dopamine transmission and the emergence of exaggerated beta oscillations in subthalamic nucleus and cerebral cortex. J. Neurosci. *28*, 4795–4806.

McCairn, K.W., and Turner, R.S. (2009). Deep brain stimulation of the globus pallidus internus in the parkinsonian primate: local entrainment and suppression of low-frequency oscillations. J. Neurophysiol. *101*, 1941–1960.

McIntyre, C.C., Savasta, M., Kerkerian-Le Goff, L., and Vitek, J.L. (2004). Uncovering the mechanism(s) of action of deep brain stimulation: activation, inhibition, or both. Clin. Neurophysiol. *115*, 1239–1248.

McIntyre, C.C., Frankenmolle, A.M., Wu, J., Noecker, A.M., and Alberts, J.L. (2009). Customizing deep brain stimulation to the patient using computational models. Conf. Proc. IEEE Eng. Med. Biol. Soc. *2009*, 4228–4229.

Mikos, A., Bowers, D., Noecker, A.M., McIntyre, C.C., Won, M., Chaturvedi, A., Foote, K.D., and Okun, M.S. (2011). Patient-specific analysis of the relationship between the volume of tissue activated during DBS and verbal fluency. Neuroimage *54* (*Suppl 1*), S238–S246.

Mink, J.W. (1996). The basal ganglia: focused selection and inhibition of competing motor programs. Prog. Neurobiol. *50*, 381–425.

Moran, A., and Bar-Gad, I. (2010). Revealing neuronal functional organization through the relation between multi-scale oscillatory extracellular signals. J. Neurosci. Methods *186*, 116–129.

Moro, E., Poon, Y.Y., Lozano, A.M., Saint-Cyr, J.A., and Lang, A.E. (2006). Subthalamic nucleus stimulation: improvements in outcome with reprogramming. Arch. Neurol. *63*, 1266–1272.

Moro, E., Lozano, A.M., Pollak, P., Agid, Y., Rehncrona, S., Volkmann, J., Kulisevsky, J., Obeso, J.A., Albanese, A., Hariz, M.I., et al. (2010). Long-term results of a multicenter study on subthalamic and pallidal stimulation in Parkinson's disease. Mov. Disord. *25*, 578–586.

Nambu, A., Tokuno, H., Hamada, I., Kita, H., Imanishi, M., Akazawa, T., Ikeuchi, Y., and Hasegawa, N. (2000). Excitatory cortical inputs to pallidal neurons via the subthalamic nucleus in the monkey. J. Neurophysiol. *84*, 289–300.

Nise, N.S. (2007). Design via state space. In Control Systems Engineering (Hoboken, NJ: John Wiley and Sons), pp. 636–690.

Parush, N., Tishby, N., and Bergman, H. (2011). Dopaminergic balance between reward maximization and policy complexity. Front Syst Neurosci *5*, 22.

Popovych, O.V., Hauptmann, C., and Tass, P.A. (2005). Effective desynchronization by nonlinear delayed feedback. Phys. Rev. Lett. *94*, 164102.

Raz, A., Feingold, A., Zelanskaya, V., Vaadia, E., and Bergman, H. (1996). Neuronal synchronization of tonically active neurons in the striatum of normal and parkinsonian primates. J. Neurophysiol. *76*, 2083–2088.

Raz, A., Vaadia, E., and Bergman, H. (2000). Firing patterns and correlations of spontaneous discharge of pallidal neurons in the normal and the tremulous 1-methyl-4-phenyl-1,2,3,6-tetrahydropyridine vervet model of parkinsonism. J. Neurosci. *20*, 8559–8571.

Redmond, D.E., Jr., Roth, R.H., and Sladek, J.R., Jr. (1985). MPTP produces classic parkinsonian syndrome in African green monkeys. Soc. Neurosci. Abstr. *11*, 166.

Rouse, A.G., Stanslaski, S.R., Cong, P., Jensen, R.M., Afshar, P., Ullestad, D., Gupta, R., Molnar, G.F., Moran, D.W., and Denison, T.J. (2011). A chronic generalized bi-directional brain-machine interface. J. Neural Eng. *8*, 036018.

Stanslaski, S., Cong, P., Carlson, D., Santa, W., Jensen, R., Molnar, G., Marks, W.J., Jr., Shafquat, A., and Denison, T. (2009). An implantable bi-directional brain-machine interface system for chronic neuroprosthesis research. Conf. Proc. IEEE Eng. Med. Biol. Soc. *2009*, 5494–5497.

Tass, P.A. (2003). A model of desynchronizing deep brain stimulation with a demand-controlled coordinated reset of neural subpopulations. Biol. Cybern. *89*, 81–88.

Tass, P., Smirnov, D., Karavaev, A., Barnikol, U., Barnikol, T., Adamchic, I., Hauptmann, C., Pawelcyzk, N., Maarouf, M., Sturm, V., et al. (2010). The causal relationship between subcortical local field potential oscillations and Parkinsonian resting tremor. J. Neural Eng. *7*, 16009.

Timmermann, L., Gross, J., Dirks, M., Volkmann, J., Freund, H.J., and Schnitzler, A. (2003). The cerebral oscillatory network of parkinsonian resting tremor. Brain *126*, 199–212.

Uhlhaas, P.J., and Singer, W. (2006). Neural synchrony in brain disorders: relevance for cognitive dysfunctions and pathophysiology. Neuron *52*, 155–168.

Uhlhaas, P.J., and Singer, W. (2010). Abnormal neural oscillations and synchrony in schizophrenia. Nat. Rev. Neurosci. *11*, 100–113.

van Rooden, S.M., Colas, F., Martínez-Martín, P., Visser, M., Verbaan, D., Marinus, J., Chaudhuri, R.K., Kok, J.N., and van Hilten, J.J. (2011). Clinical subtypes of Parkinson's disease. Mov. Disord. *26*, 51–58.

Vitek, J.L. (2002). Mechanisms of deep brain stimulation: excitation or inhibition. Mov. Disord. *17* (*Suppl 3*), S69–S72.

Vitek, J.L. (2008). Deep brain stimulation: how does it work? Cleve. Clin. J. Med. *75* (*Suppl 2*), S59–S65.

Volkmann, J., Moro, E., and Pahwa, R. (2006). Basic algorithms for the programming of deep brain stimulation in Parkinson's disease. Mov. Disord. *21* (*Suppl 14*), S284–S289.

Weaver, F.M., Follett, K., Stern, M., Hur, K., Harris, C., Marks, W.J., Jr., Rothlind, J., Sagher, O., Reda, D., Moy, C.S., et al; CSP 468 Study Group. (2009). Bilateral deep brain stimulation vs best medical therapy for patients with advanced Parkinson disease: a randomized controlled trial. JAMA *301*, 63–73.

Weinberger, M., Hutchison, W.D., and Dostrovsky, J.O. (2009). Pathological subthalamic nucleus oscillations in PD: can they be the cause of bradykinesia and akinesia? Exp. Neurol. *219*, 58–61.

Wichmann, T., and DeLong, M.R. (2006). Basal ganglia discharge abnormalities in Parkinson's disease. J. Neural Transm. Suppl. 21–25.

Zaidel, A., Arkadir, D., Israel, Z., and Bergman, H. (2009). Akineto-rigid vs. tremor syndromes in Parkinsonism. Curr. Opin. Neurol. *22*, 387–393.